AIAA JOURNAL
Vol. 48, No. 6, June 2010

Bifurcation Prediction of Large-Order Aeroelastic Models

K. J. Badcock* and M. A. Woodgate†
University of Liverpool, England L69 3BX, United Kingdom

DOI: 10.2514/1.40961

Computational aeroelasticity has become an active area of research in the past decade. Effort has been put into coupling between computational fluid dynamic and finite element solvers and into model reduction to make the resulting simulations more useful for practical analysis. This paper is the latest in a series that describe research toward making eigenvalue-based stability analysis routine for large-scale computational-fluid-dynamic-based semidiscrete systems. The particular contribution of this paper is to formulate the problem in a framework that exploits the Schur complement. This effectively allows the different parts of the system Jacobian to be treated in a decoupled way, with the final result being a small nonlinear eigenvalue problem for the stability analysis. The calculation of this small system can be done robustly in parallel. Results to illustrate the performance of the method are presented for model wings and full aircraft test cases.

Nomenclature

A	=	Jacobian matrix
p	=	eigenvector
$\mathbf{R}$	=	residual vector of the fluid and/or structural model
S	=	Schur complement matrix
$\mathbf{w}$	=	vector of fluid and/or structural unknowns
λ	=	eigenvalue
μ	=	bifurcation parameter (altitude)

Subscripts

f	=	fluid model
s	=	structural model
0	=	equilibrium

I. Introduction

THE system derived from coupling a computational fluid dynamics (CFD) code with a finite element method (FEM) can be used in different ways to simulate the aeroelastic behavior of an aircraft. The advancement of the coupled system in time can give information about the response to an initial disturbance, and hence the system stability [1]. This approach, however, must carry the cost of the unsteady CFD simulation and is unattractive for this reason, particularly when a large parameter space must be investigated. An additional drawback is that the time-domain approach does not fit with the conventional approach to aircraft aeroelasticity, which is to examine the influence of the aerodynamics on the structural normal modes and to look at the interaction of the aeroelastic modes.

An alternative is to use the coupled system to generate response information to forced inputs. The information is then used to set up a data-driven model [2]. The data-driven model is used to investigate the system free response at much lower cost than the full-order system. However, the data-driven models are only applicable within the support of the data used to generate them. They are often formulated to be linearizations about a mean state, which will more than likely depend on the system parameters as well. If this is taken into account, then the calculations required to generate the model can be quite extensive, driving up the total cost of the method.

An alternative is to stick with the full-order system but to exploit some property of the dynamics to reduce the computational cost. One example is the harmonic balance method that assumes that the unstable response of the system is at a set of discrete frequencies (typically one) [3]. The assumed harmonic content is used to reduce the cost of calculations to the equivalent of a few steady-state calculations for an assumed response frequency.

The approach used in the current paper is to view the problem of computing flutter onset as a stability problem for a steady state of the coupled system. Assuming a Hopf Bifurcation, stability is lost when the system Jacobian matrix has a pair of eigenvalues that cross the imaginary axis. The idea is to compute when this happens at a computational cost much less than time-domain analysis.

This was first attempted for a symmetric airfoil free to move in pitch and plunge [4]. The coupled system of equations was augmented by an equation for a purely imaginary eigenvalue. The augmented system was solved using Newton's method. Approximations were made to make the direct solution of the linear system for the updates more tractable. Unfortunately these approximations degraded the convergence and robustness of the method.

These problems were overcome by using an iterative linear solver [5]. The method was extended to three-dimensional cases in [6]. A problem with the augmented system is that the Newton iterations require the second Jacobian in the coefficient matrix. It is unfeasible to form this matrix explicitly. For symmetric problems the calculation of the steady state is independent of the dynamic pressure and the equilibrium can be calculated separately from the behavior of the eigensystem [4–6]. In this case, the second Jacobian is not needed. However, in the general case, the steady state and the eigensystem must be calculated in a coupled manner.

To overcome this problem, the classical shifted inverse power method was adapted to track eigenvalues as the dynamic pressure changes [7]. This method solves a system very similar to the augmented system, but the steady state can be updated for each value of the dynamic pressure before the eigenvalue is calculated. The output of the method is a locus of the aeroelastic system eigenvalues. In a manner identical to classical linear flutter analysis, the frequency and damping values can be tracked, and the value of dynamic pressure where the damping is lost for any mode can be located.

There were two limitations with the method as presented. First, a parallel implementation was needed to deal with realistically sized models. Second, the mode tracking was not sufficiently robust. The central computational problem involved with calculating stability through eigenvalues is that the linear system (at least in the approaches based on tracking individual eigenvalues through shift

Presented as Paper 1820 at the 49th AIAA/ASME/ASCE/AHS/ASC Structures, Structural Dynamics, and Materials Conference, Schaumburg, IL, 7–10 April 2008; received 12 September 2008; accepted for publication 28 February 2010.

*Professor, Computational Fluid Dynamics Laboratory, Flight Sciences and Technology, Department of Engineering; K.J.Badcock@liverpool.ac.uk (Corresponding Author).

†Research Assistant, Computational Fluid Dynamics Laboratory, Flight Sciences and Technology, Department of Engineering.

and invert methods) invariably ends up being increasingly ill-conditioned as the eigenvalue is approached. The linear system is then very difficult to solve, particularly when extra approximations are needed to obtain a preconditioner that can be calculated in parallel.

The current paper aims to avoid the problem of solving linear systems with a coefficient matrix that is almost singular through a reformulation using the Schur complement. The reformulation leads to a small nonlinear eigenvalue problem that can be solved over an altitude range at very low computational cost. In the process, the mode-tracking problem is solved, since very small increments of altitude can be used. This paper continues with a brief summary of the underlying coupled CFD-FEM system. The Schur complement eigenvalue formulation is then described. Results are given for four test problems to illustrate the performance of the method. The paper finishes with conclusions.

II. Coupled Formulation

The semidiscrete form of the coupled CFD-FEM system is written as

$$\frac{\mathrm{d}\mathbf{w}}{\mathrm{d}t} = \mathbf{R}(\mathbf{w}, \mu) \tag{1}$$

where

$$\mathbf{w} = [\mathbf{w}_f, \mathbf{w}_s]^T \tag{2}$$

is a vector containing the fluid unknowns $\mathbf{w}_f$ and the structural unknowns $\mathbf{w}_s$, and

$$\mathbf{R} = [\mathbf{R}_f, \mathbf{R}_s]^T \tag{3}$$

is a vector containing the fluid residual $\mathbf{R}_f$ and the structural residual $\mathbf{R}_s$. The residual also depends on a parameter μ (in this paper μ is altitude), which is independent of $\mathbf{w}$. An equilibrium $\mathbf{w}_0(\mu)$ of this system satisfies $\mathbf{R}(\mathbf{w}_0, \mu) = \mathbf{0}$.

The stability of equilibria of Eq. (1) is determined by eigenvalues of the Jacobian matrix $A = \partial\mathbf{R}/\partial\mathbf{w}$. In the examples considered in the current paper, stability is lost through a Hopf bifurcation, where a complex conjugate pair of eigenvalues of A crosses the imaginary axis.

The calculation of the Jacobian A is most conveniently done by partitioning the matrix as

$$A = \begin{bmatrix} \frac{\partial \mathbf{R}_f}{\partial \mathbf{w}_f} & \frac{\partial \mathbf{R}_f}{\partial \mathbf{w}_s} \\ \frac{\partial \mathbf{R}_s}{\partial \mathbf{w}_f} & \frac{\partial \mathbf{R}_s}{\partial \mathbf{w}_s} \end{bmatrix} = \begin{bmatrix} A_{ff} & A_{fs} \\ A_{sf} & A_{ss} \end{bmatrix} \tag{4}$$

The block A_{ff} is a large sparse matrix derived by differentiating the CFD residual (built up from fluxes calculated using Osher's method, which is differentiable everywhere) with respect to the CFD cell values. This is a nontrivial task, but has nonetheless been done analytically. The term A_{fs} arises from the dependence of the CFD residual on the mesh motion and speeds, which in turn depend on the structural solution. These terms are currently evaluated using finite differences. The term A_{sf} is due to the dependence of the generalized forces on the surface pressures. Finally, A_{ss} is the Jacobian of the structural equations with respect to the structural unknowns. The details of the Jacobian calculation are given in [5,6]. Note that all four matrices depend on the aerostatic solution. In the current paper, this solution is assumed to be independent of μ. The general case in which this is not true is discussed in the Conclusions.

In the current work, and as is conventional in aircraft aeroelasticity, the structure is modeled by a small number of modes, and so the number of the fluid unknowns is far higher than the structural unknowns. This means that the Jacobian matrix has a large, but sparse, block A_{ff} surrounded by thin strips for A_{fs} and A_{sf}.

III. Schur Complement Eigenvalue Solver

The stability calculation is formulated as an eigenvalue problem. The task is to find the eigenvalues of the matrix in Eq. (4), which have the most positive real part. To focus this search, the aeroelastic eigenvalue problem can be viewed as tracking the structural normal modes when they are under the influence of the fluid. This follows the well established approach for linear analysis. The structural eigenvalues are those of the block A_{ss}, which has the dimension $2n$, where n is the number of normal modes retained from the structural model.

Now, write the coupled system eigenvalue problem as

$$\begin{bmatrix} A_{ff} & A_{fs} \\ A_{sf} & A_{ss} \end{bmatrix} \mathbf{p} = \lambda \mathbf{p} \tag{5}$$

where $\mathbf{p}$ and λ are the complex eigenvector and eigenvalue, respectively. Partition the eigenvector as

$$\mathbf{p} = [\mathbf{p}_f, \mathbf{p}_s]^T \tag{6}$$

It can be shown [8] that the eigenvalue λ (assuming it is not an eigenvalue of A_{ff}) satisfies the nonlinear eigenvalue problem:

$$S(\lambda)\mathbf{p}_s = \lambda \mathbf{p}_s \tag{7}$$

where $S(\lambda) = A_{ss} - A_{sf}(A_{ff} - \lambda I)^{-1}A_{fs}$. Looking to this nonlinear eigenvalue problem, the matrix $S(\lambda)$ has the following features. First, it is the sum of the structural matrix and a second term (referred to here as the correction matrix), which arises from the coupling with the fluid model. As the coupling is reduced to zero, through increasing the altitude, the structural matrix is recovered and an eigenvalue of the uncoupled system is then obtained. Second, the correction matrix depends on the eigenvalue, producing a *frequency matching* with the aerodynamics as part of the solution method. Third, the inverse of the matrix $A_{ff} - \lambda I$ is required, and importantly, λ is not an eigenvalue of A_{ff}, avoiding the ill-conditioning that would arise if this was not the case.

The nonlinear Eq. (7) is solved using Newton's method. Each iteration requires the formation of the residual and its Jacobian matrix. The formation of the correction matrix is required to form the Jacobian matrix. This can be achieved through $2n$ solutions of a linear system against $A_{ff} - \lambda I$, one for each column of A_{fs}. These solutions are then multiplied against A_{sf}. Now, for each value of the bifurcation parameter, there are n solutions of the nonlinear system in Eq. (7), and so the cost of forming the correction matrix at each Newton step, for each solution and for a range of parameters becomes too high. To overcome this the expansion,

$$(A_{ff} - \lambda I)^{-1} = A_{ff}^{-1} + \lambda A_{ff}^{-1}A_{ff}^{-1} + \lambda^2 A_{ff}^{-1}A_{ff}^{-1}A_{ff}^{-1} + \cdots \tag{8}$$

is used, where λ must be small for the series to converge. Note that this restriction can be overcome by assuming that the eigenvalue we are calculating is a small change from the eigenvalue λ_0 of A_{ss}. Then λ_0 can be used as a shift to the full system eigenvalue problem by replacing A_{ff} by $A_{ff} - \lambda_0 I$ and A_{ss} by $A_{ss} - \lambda_0$. This modifies the nonlinear eigenvalue problem in Eq. (7) by redefining

$$S(\lambda) = (A_{ss} - \lambda_0 I) - A_{sf}(A_{ff} - \lambda_0 I - \lambda I)^{-1}A_{fs}$$

Now the series approximation becomes

$$(A_{ff} - \lambda_0 I - \lambda I)^{-1} = (A_{ff} - \lambda_0 I)^{-1} + \lambda(A_{ff} - \lambda_0 I)^{-2} + \lambda^2(A_{ff} - \lambda_0 I)^{-3} + \cdot \tag{9}$$

where λ is a small change to λ_0. When the nonlinear eigenvalue problem is solved for λ, the eigenvalue of the original system is then $\lambda_0 + \lambda$.

Note that the value of λ is decoupled from the matrix inverse through the use of the series expansion. If the altitude is the bifurcation parameter, then the dynamic pressure can also be pulled out of the correction matrix as a coefficient. The nonlinear system can then be formulated in the following way:

1) Select the normal mode to be tracked; denote the eigenvalue shift as λ_0, which is the frequency of the normal mode.

2) Truncating the series expansion at two terms, calculate $(A_{ff} - \lambda_0 I)^{-1} A_{fs}$, $(A_{ff} - \lambda_0 I)^{-2} A_{fs}$. This requires $4n$ linear systems to be solved, where n is the number of normal modes retained.

3) Solve Newton's method using the correction matrix with the series expansion used to generate the left-hand side Jacobian matrix for the Schur eigenvalue problem. The right-hand side residual can be evaluated using the series expansion (referred to in this paper as the *series method*) or by one linear system solve against the matrix $(A_{ff} - \lambda_0 I - \lambda I)$ (referred to as the *nonlinear method*). The consideration here is how large λ has become. If it is small, then the series expansion can be used for the residual without incurring significant error. Results below will show that this behavior can be anticipated.

Solutions of the nonlinear eigenvalue problem are traced out for values of the bifurcation parameter (the altitude in this paper). If the series method is used, then very small increments of the parameter can be used, since once the correction matrix is generated, the cost of solving the nonlinear eigenvalue problems is almost negligible. On the other hand, if the nonlinear method is used, then the series solutions can act as an initial guess for the nonlinear method, which is solved at larger parameter increments. If the Newton method fails to converge, then this indicates that the series approximation has become too poor to drive convergence, and the correction matrix can be regenerated with the best approximation to the eigenvalue at the current altitude as the new shift. In the cases computed for this paper, this was never necessary. The two options have both been found to give very robust mode tracking.

IV. Parallel Implementation of the Linear Solver

The sparse linear system to generate the correction matrix is solved using the generalized conjugate residual (GCR) algorithm [9]. The crucial aspect of the solution is the preconditioning. Some options previously considered are discussed in [10]. In summary,

1) The block incomplete upper/lower factorization, with one or two levels of fill-in, of the matrix $A^*_{ff} - \lambda_0 I$ is used.

2) Here, A^* is an average of the Jacobian matrix derived when using the first-order spatial discretization for the CFD residual and the matrix A_{ff} (based on the second-order spatial scheme). Experiments have shown that the factorization based on A_{ff} makes a poor preconditioner, possibly due to the factorization being unstable.

3) The factorization is done in terms of complex variables, which appears to improve the quality of the preconditioner.

4) The terms in the coefficient matrix of the linear system are included for the matrix-vector products, and so the converged solution of the GCR iterations will not be polluted by approximations made for the preconditioning.

5) For parallel calculations, the factorization is blocked on each processor. It is possible to improve on this by using an alternative preconditioning with inner iterations [11].

Previous experience with solving a linear system against the shifted form of the coupled matrix given in Eq. (4) was that the preconditioning described above is inadequate as the number of processors increases. This is likely to be because the matrix becomes singular as the shift tends toward an eigenvalue. In the Schur formulation this problem is avoided, and in all of the applications computed for this paper, the linear system was solved (defined as

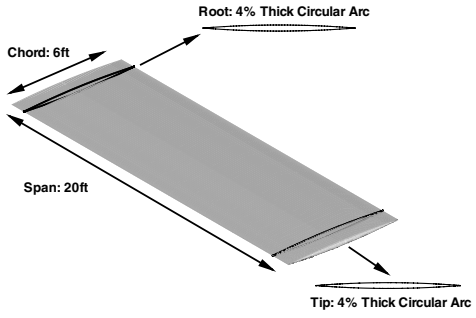

Summary of Geometry

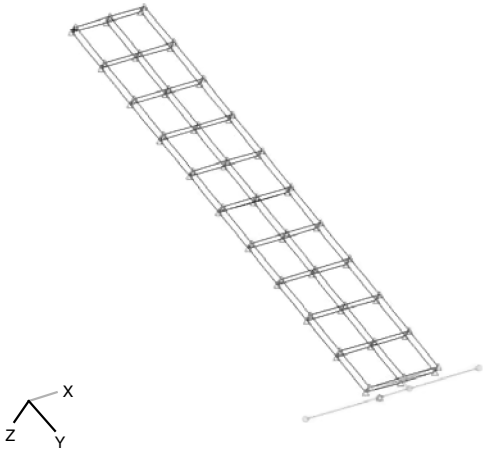

FE mesh

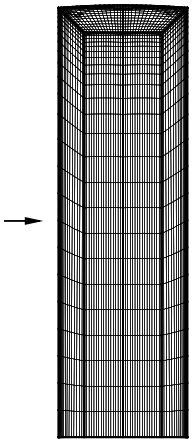

surface CFD grid

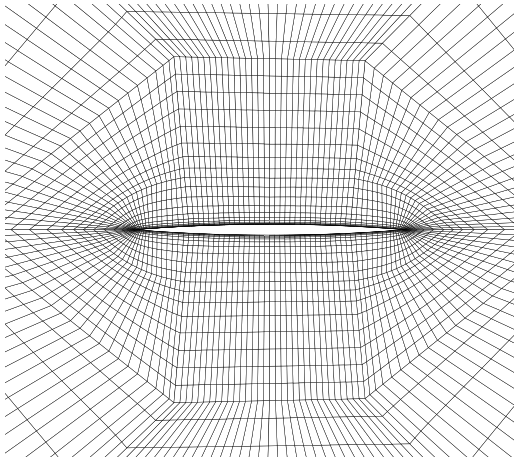

slice from volume CFD grid

Fig. 1 Views of geometry, FEM, and CFD grids for a Goland wing.

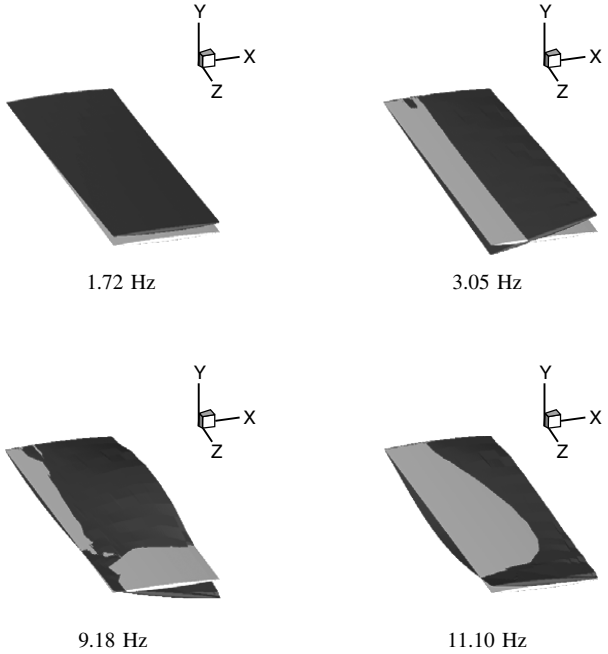

Fig. 2 Mode shapes mapped to the CFD surface grid for a Goland wing.

driving the initial residual down by seven orders of magnitude), on average, in about 100 steps and never more than 220 steps.

V. Results

A. Goland Wing

The Goland wing, shown in Fig. 1, has a chord of 6 ft and a span of 20 ft. It is a rectangular cantilevered wing with a 4% thick parabolic section. The structural model follows the description given in [12] and is shown in Fig. 1. The CFD grid is block structured and uses an O-O topology. This allows points to be focused in the tip region, which is most critical for the aerodynamic contribution to the aeroelastic response. The fine grid has 236,000 points and a coarse level was extracted from this grid, which has 35,000 points. Views of the fine grid are shown in Fig. 1. Four mode shapes were retained for the aeroelastic simulation. The mapped modes on the CFD surface grid are shown in Fig. 2.

The test case has a tip store in the structural model. This case is interesting because it leads to a bucket of shock-induced limit cycle oscillation for a freestream Mach number of around 0.92. This was investigated in [7], which also included a review of previous studies and the prediction of the LCO amplitude using a model reduction based on the critical eigenvector. The Goland wing is very flexible and leads to instability within the flight envelope at all high subsonic freestream Mach numbers. The case is particularly useful in the current work to test the validity of the series expansion when there are significant changes in the aeroelastic eigenvalue as the altitude is reduced.

The correction matrices were first calculated, for a number of Mach numbers in the range 0.3 to 0.97, at the highest of the altitude range considered (−10 to 30,000 ft). All calculations have a 0 deg angle of attack. The matrices were calculated on the coarse and fine grids, with the fine grid calculations being done in parallel on eight processors. The convergence of the linear solver during these calculations was good for all cases, with around 30 linear solver steps per column calculated required on the coarse grid and around 80 on the fine grid. The eigenvalues were then traced based on these matrices. Four different types of behavior were observed and are illustrated in Fig. 3. First, at low Mach numbers (such as Mach 0.3 in Fig. 3), no instability is predicted in the altitude range. This is in agreement (as expected) with linear predictions obtained by running NASTRAN. Second, as the Mach number is increased the first bending and torsion modes interact, with the real part of the bending mode eigenvalue becoming positive within the altitude range. An example of this behavior at Mach 0.8 is shown in Fig. 3. The quantitative agreement with NASTRAN is also good for this behavior as indicated on the plot of the real part. This is expected because the instability is not yet driven by shock waves. With increasing freestream Mach number a strong shock develops toward the trailing edge of the wing, as shown in Fig. 3 at Mach 0.92. Now the torsion mode is unstable at all points in the altitude range, as shown in the plot of variation of the real part of the eigenvalue. At this point NASTRAN also predicts that all modes are unstable, although this must be for reasons other than the presence of shock waves. Finally, at higher freestream Mach numbers the shock reaches the trailing edge and the wing recovers stability at higher altitude (Mach 0.97 in the figure). The flutter mechanism changes with an interaction

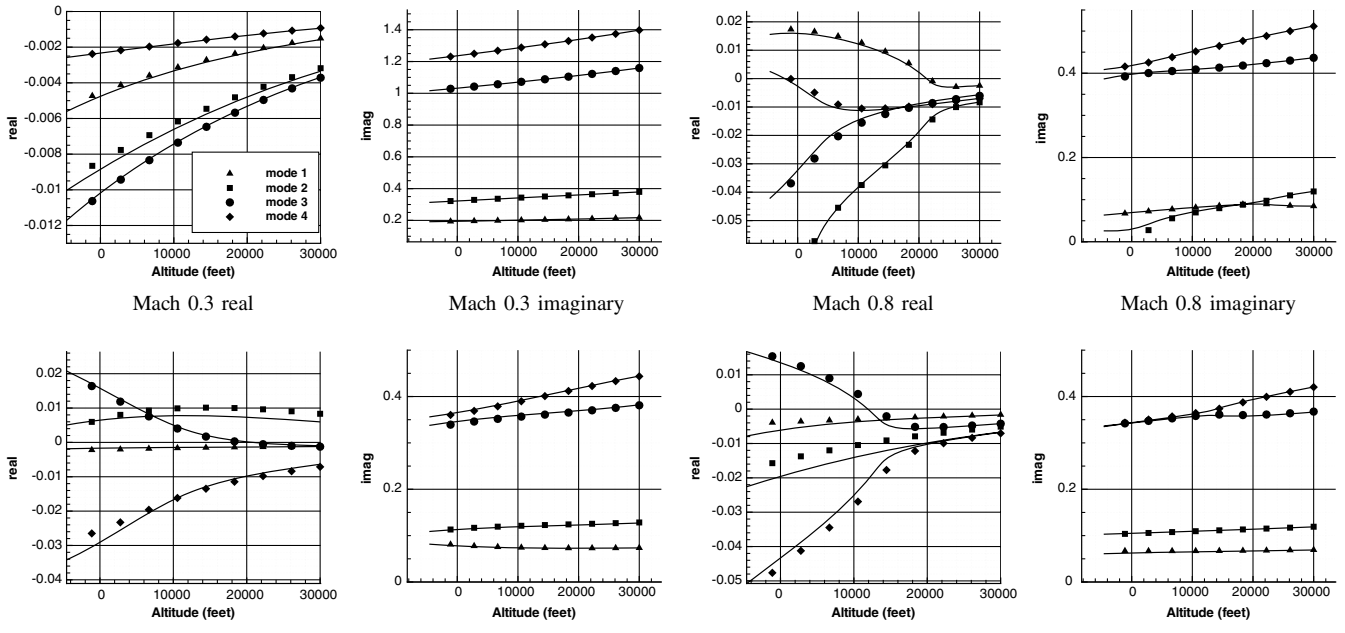

Fig. 3 Variation of real and imaginary parts with altitude for a Goland wing, together with surface pressure distributions showing the shock wave development.

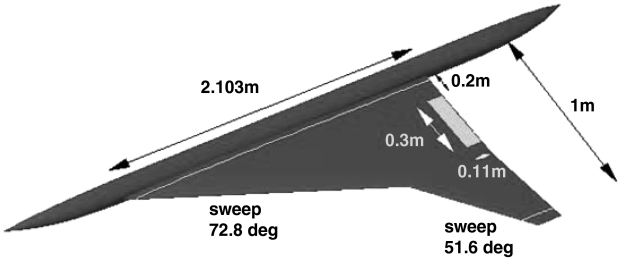

Fig. 4 SST geometry.

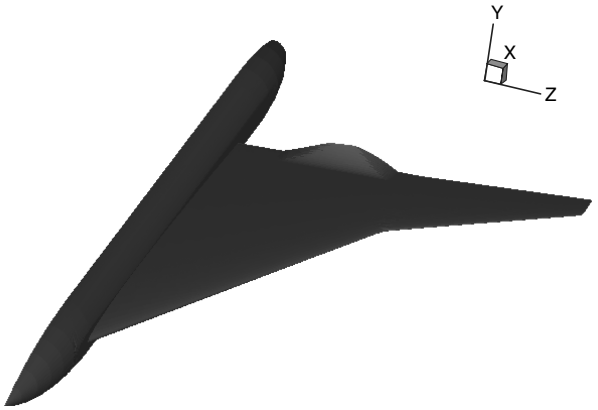

Fig. 5 Deflected control surface defined on the CFD surface grid for the SST configuration.

observed between the second torsion and bending modes. NASTRAN continues to predict instability at all points in the altitude range.

The consistency of the results was evaluated in three ways. First, comparisons with NASTRAN showed agreement at low freestream Mach numbers as expected, since the aerodynamic predictions from the Euler equations and the potential theory should be similar in the absence of significant nonlinear compressible effects. Second, the eigenvalues traced for the fine (solid lines) and coarse (dashed lines) grids are both shown in Fig. 3 and are in good agreement. Finally, and most importantly, the influence of the series expansion on the accuracy of the predicted eigenvalues was considered. This was done by solving the Schur eigenvalue problem using an evaluation of $S(\lambda)$, by solving a linear system against $A_{ff} - \lambda I$, rather than using the series expansion given in Eq. (9) to simplify this computational task. The results from the former approach are plotted using points in Fig. 3, labeled as *nonlinear*. Even with significant changes in the eigenvalue real and imaginary parts over the altitude range, the predictions using the series expansion are shown to be excellent for this case.

For the fine grid and on eight processors, the time required to calculate a steady state was 11 min, the time to form the correction matrix was 137 min (with the eigenvalue curves over the whole altitude range, then computed at virtually no extra cost after this), and the time to compute the four sets of eigenvalues using the nonlinear method at eight values of altitude is an additional 202 min, with an average of three iterations per eigenvalue. The necessary wall clock time on eight processors to compute one flutter point is therefore 13.5 times the cost of a steady-state solution.

B. Supersonic Transport Control Surface Buzz

The second test case is based on the transonic aeroelastic experiments performed at the National Aerospace Laboratory of Japan [13]. One of the motivations for the experiments was to generate a set of results against which aeroelastic codes could be validated. For this reason, along with the unsteady pressure distribution over the wing, the dynamic deformation, and unsteady force coefficients were also measured. The supersonic transport (SST) arrow wing is a cranked double delta with a root chord of 7.01 ft. A half-model was used in the experiments with a semispan of 3.33 ft. The section profile is a NACA 0003. The inboard delta has a sweep angle of 72.8° and outboard the sweep is 51.6°. The trailing-edge flap starts at 20% half-span and terminates at 50% half-span, with a flap chord of 0.367 ft. The geometry is summarized in Fig. 4.

Experimental pressure and deformation data were collected at transonic Mach numbers, low angles of attack and for forced flap motions at various amplitudes and frequencies. These data were used to investigate the use of a blended flap treatment [14], including validation against measurements for the unsteady pressures and dynamic structural response from forced flat motions. Evaluation was made for the structural response and the unsteady aerodynamics resulting from forced flap motions. This work was extended by Rampurawala [15] to investigate shock-induced buzz using time-domain analysis. In the current paper, the eigenvalues of the system are used to compute the onset Mach number for buzz.

For the CFD grid, a C-type grid topology is used over the wing leading edge, the wing tip, and around the fuselage. The blocks at the trailing edge are of H-type. Points are clustered around the trailing edge and the flap region where a shock is likely to develop and move. The grid has 234,000 points, with the gap between the flap edges and the wing blended over [14].

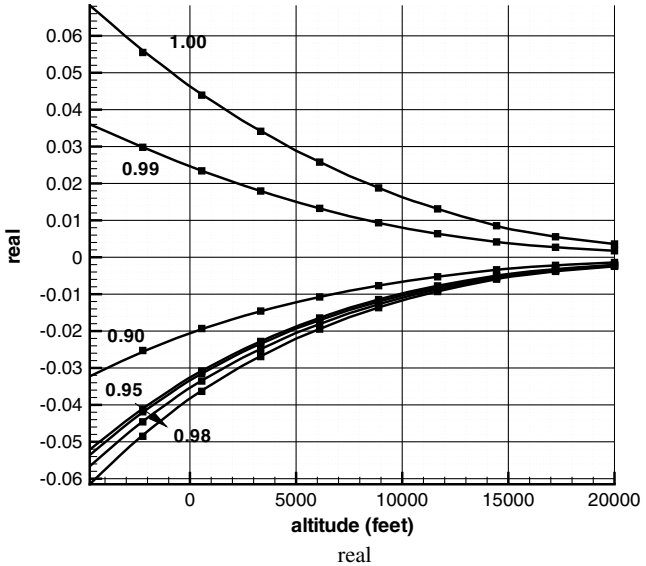

real

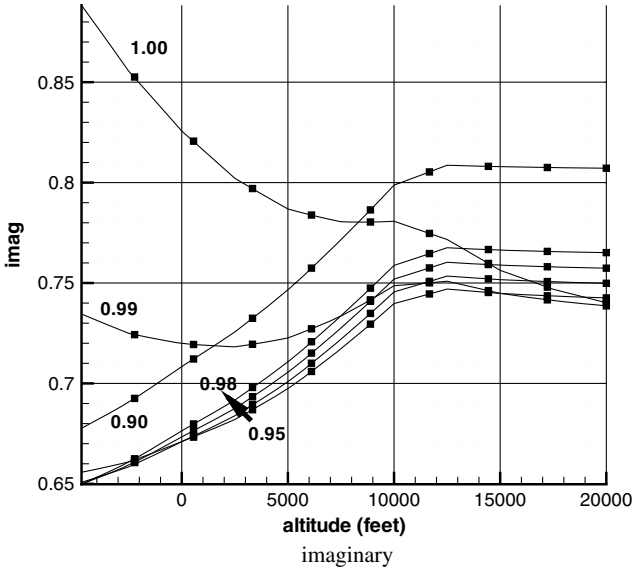

imaginary

Fig. 6 SST configuration.

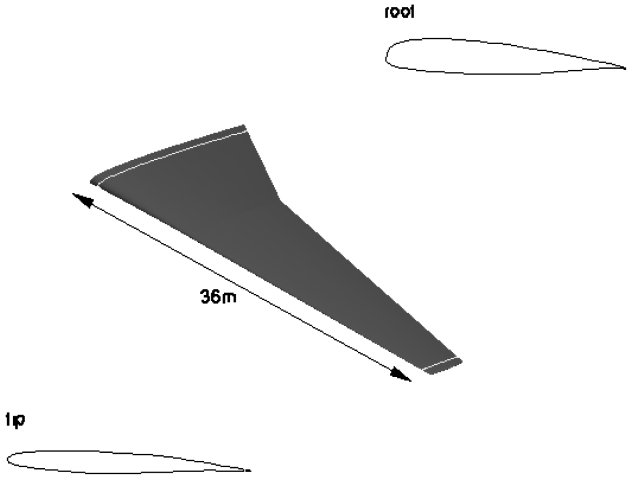

Fig. 7 MDO wing geometry.

The structure of the SST was modeled as a 2-D plate. The flap is modeled as a separate rigid plate attached to the main wing through springs. The spring stiffness constant was adjusted to give a flap frequency of 16.2 Hz, which is within the realistic frequency range of a mechanically constrained trailing-edge control surface. A plot of the control surface deflection is shown in Fig. 5. This is defined on the CFD surface grid, and indicates the blending treatment used. The flap mode was the only one retained for the current calculations.

Previously computed time-domain responses for the control surface [15] showed that in the freestream Mach number range 0.9–0.98 a shock moves onto the control surface and a limit cycle oscillation is established. The precise onset Mach number depends on the magnitude of the initial disturbance, and whether this is enough to move a shock from ahead of the hinge line over the control surface. The analysis used in the current paper, which is a linear stability analysis about a nonlinear steady state, is unable to predict this effect, which would require a nonlinear stability analysis. All calculations in the current paper were run at a 0 deg zero angle of attack.

The altitude range used was −16, 667 to 66,667 ft. The eigenvalue associated with the flap mode was traced through this altitude for Mach numbers of 0.9 and then 0.95–1.0 in steps of 0.01. The resulting plots of the real and imaginary parts is shown in Fig. 6. There are two distinct cases observed. First, for Mach numbers below 0.98, the mode is damped at all values of altitude. In contrast, at Mach 0.99 and 1.00, the mode is undamped at all values of altitude. At Mach 0.99 the shock moves onto the control surface in the steady-state solution.

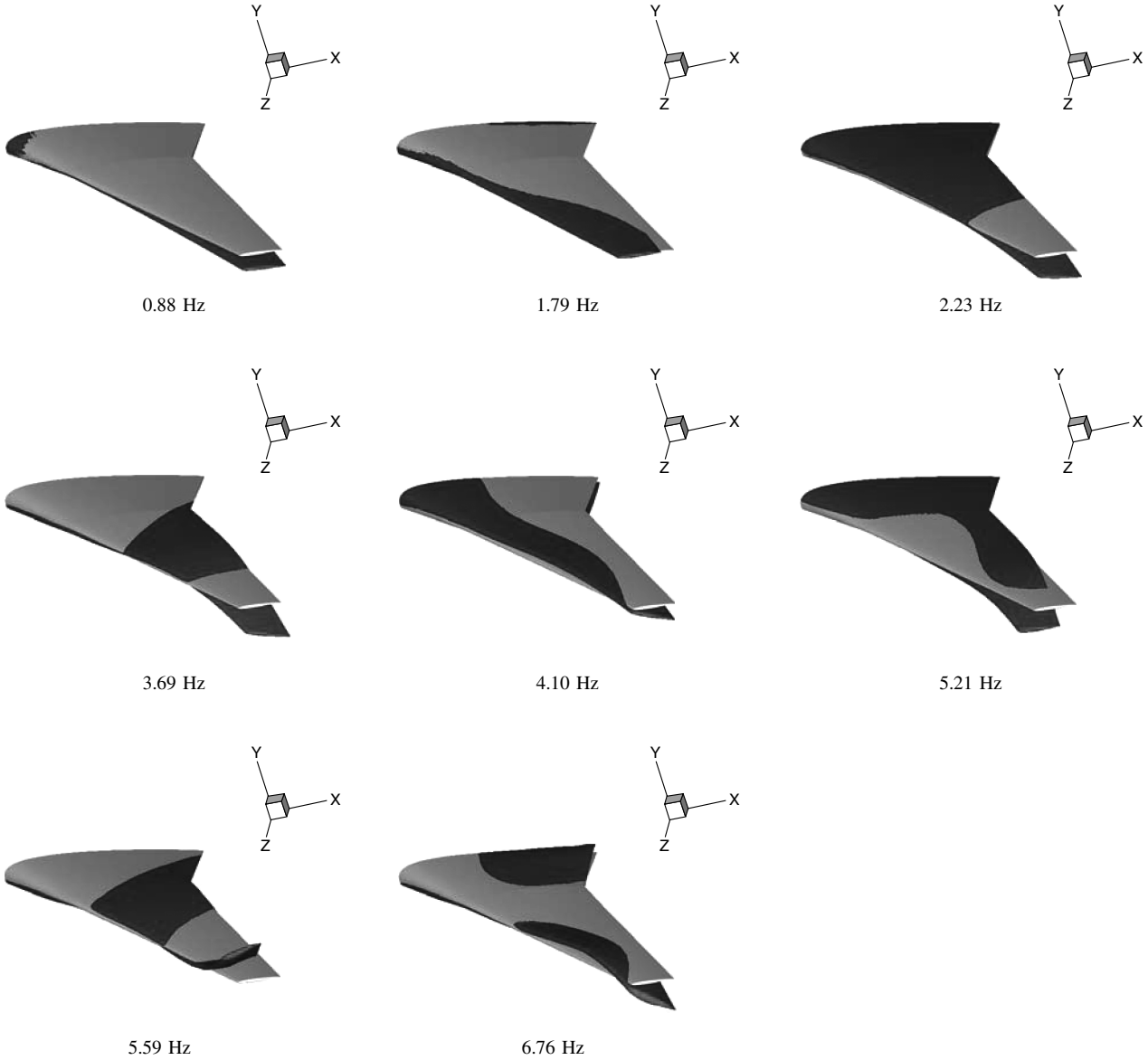

Fig. 8 Modes shapes defined on the CFD surface grid for the MDO wing.

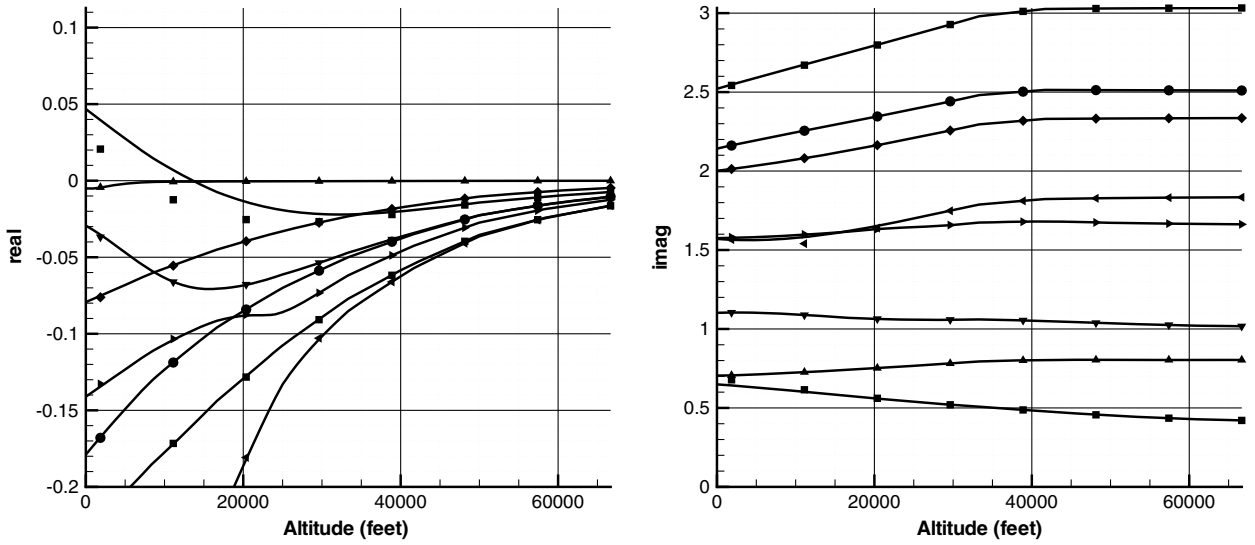

real imaginary

Fig. 9 MDO configuration.

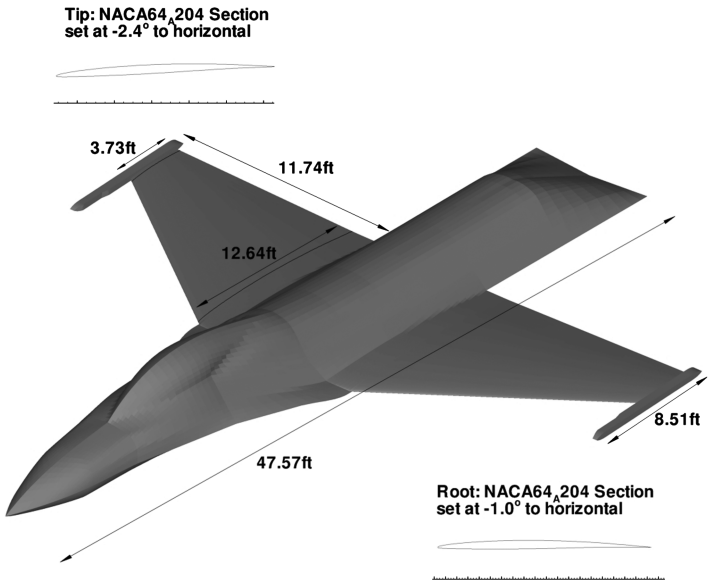

Summary of Geometry

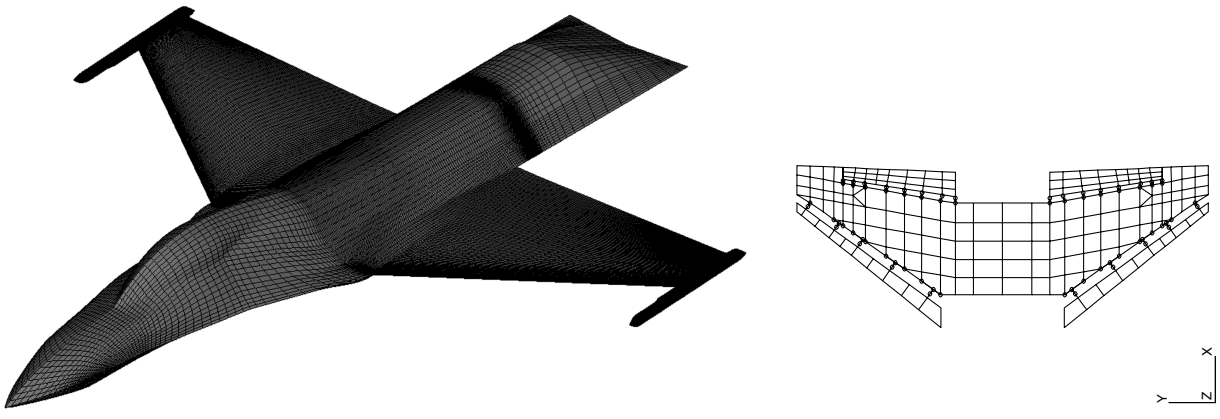

CFD surface grid FE Grid

Fig. 10 Generic fighter geometry and surface CFD and FEM grids.

Again the predictions using the series (lines) and nonlinear (dots) methods were compared and are in excellent agreement (see Fig. 6). These calculations were run on eight processors; the cost of calculating the steady state was 14 min, and the cost of generating the correction matrix was 9 min. The nonlinear solution at eight values of altitude required 49 min for 23 nonlinear steps (roughly three per eigenvalue). Hence, for this case, to compute the critical Mach number required an equivalent computational cost of 11.5 steady solves (i.e. 7 M numbers times a cost of 1.64 steady solves at each Mach number).

C. Transport Wing

The multidisciplinary design optimization (MDO) wing is a commercial transport wing, with a span of 120 ft, designed to fly in the transonic regime [16,17]. The profile is a thick supercritical section. The geometry is summarized in Fig. 7. The structure is modeled as a wing box running down the central portion of the wing. The problems of mapping this reduced planform to the full planform CFD model are considered in [18]. The CFD grid used has 81,000 points and is shown in Fig. 7. Results generated using the inverse power method to track eigenvalues were previously shown [7]. In the current work eight modes are retained and the mapped modes on the fluid surface grid are shown in Fig. 8.

The feature of this test case is the larger number of modes. The altitude range was chosen to be 0 to 66667 ft. The first wing bending and torsion modes interact to give flutter at just below 16,667 ft at Mach 0.85 and 0 deg angle of attack, as shown in Fig. 9. Again the series and nonlinear predictions are compared and this time show some discrepancy as the bending mode loses damping. However, for all modes there is good qualitative and quantitative agreement. These results suggest that a good strategy would be to compute the eigenvalues using the series method, and then to check only the mode that is critical using the nonlinear approach. Note that no aerostatic deflection was included for these results.

The steady calculation took 22 min on eight processors, and the correction matrix was generated in a total of 95 min for the eight modes. The time for the steady-state solution is high for this case, because smaller Courant–Friedrichs–Lewy numbers were required. The nonlinear solution required an average of three steps per eigenvalue, for a total of 72 min using eight values of altitude for each mode. Hence, in this case, the flutter points required around 5 times the cost of a steady-state solution.

D. Generic Fighter Model

Finally, the Schur method is exercised on a model approximating a full aircraft. The intention here is to show that the method can scale to models of the size required for the inviscid analysis of real aircraft. The generic fighter was built on data publicly available for the F-16 aircraft, since this has been the subject of much interest from an aeroelastic viewpoint. The approach was to establish a test case that is recognizable as an aircraft, and it obviously cannot be representative of the actual behavior of the F-16.

The geometry is summarized in Fig. 10. A fuselage, wing and tip launcher were included as the minimum components required. The wing has a NACA64A204 section and is twisted nose-down 2.3 deg from the root to the tip. The aircraft dimensions have been roughly based on the F-16.

A block structured grid was generated that has 890,000 points and 240 blocks for the full configuration. The full-span grid was obtained by reflecting a half-span grid. The surface grid is shown in Fig. 10 and shows that the points are concentrated on the wing that contributes most to the aeroelastic response.

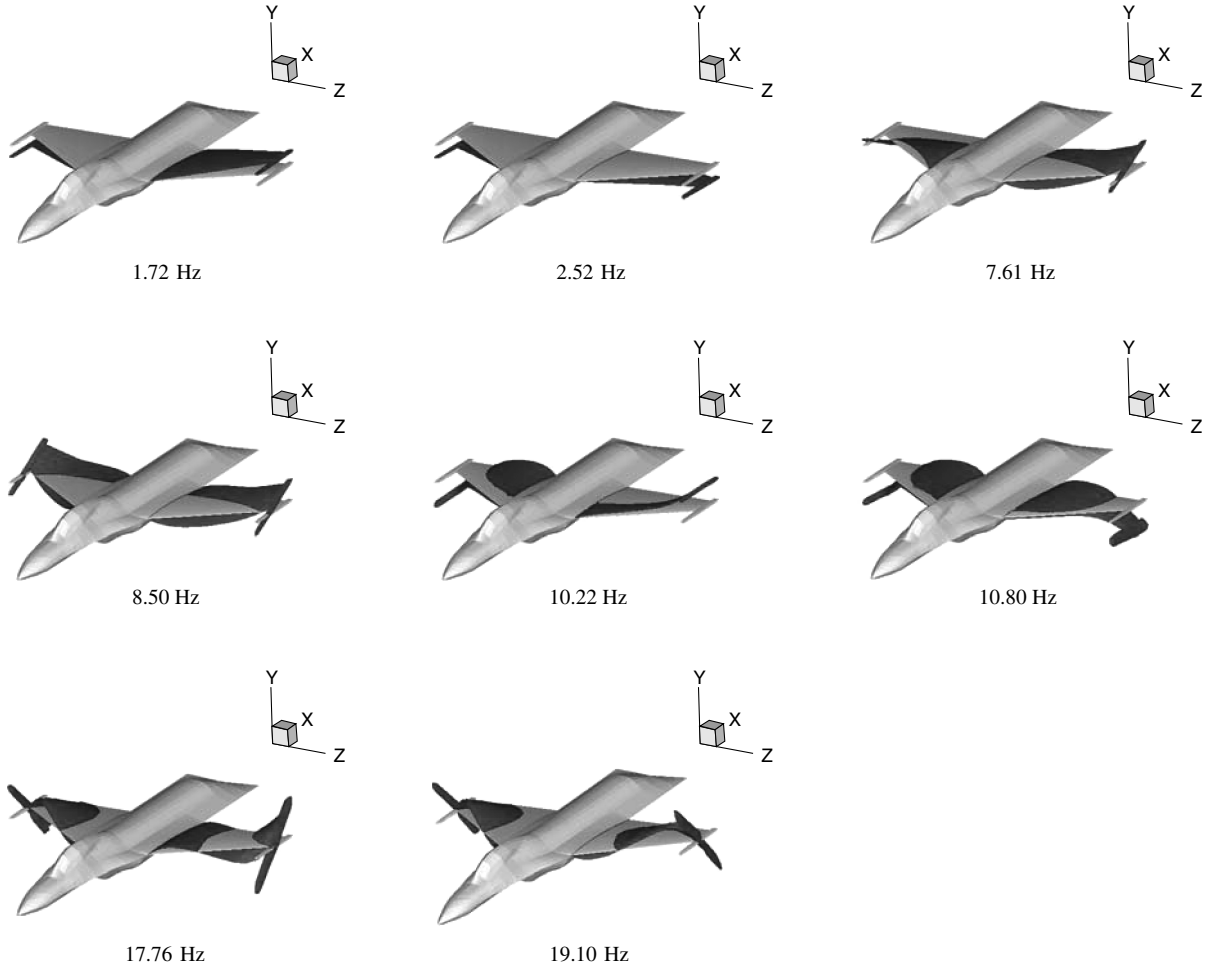

Fig. 11 Modes shapes defined on the CFD surface grid for the generic fighter.

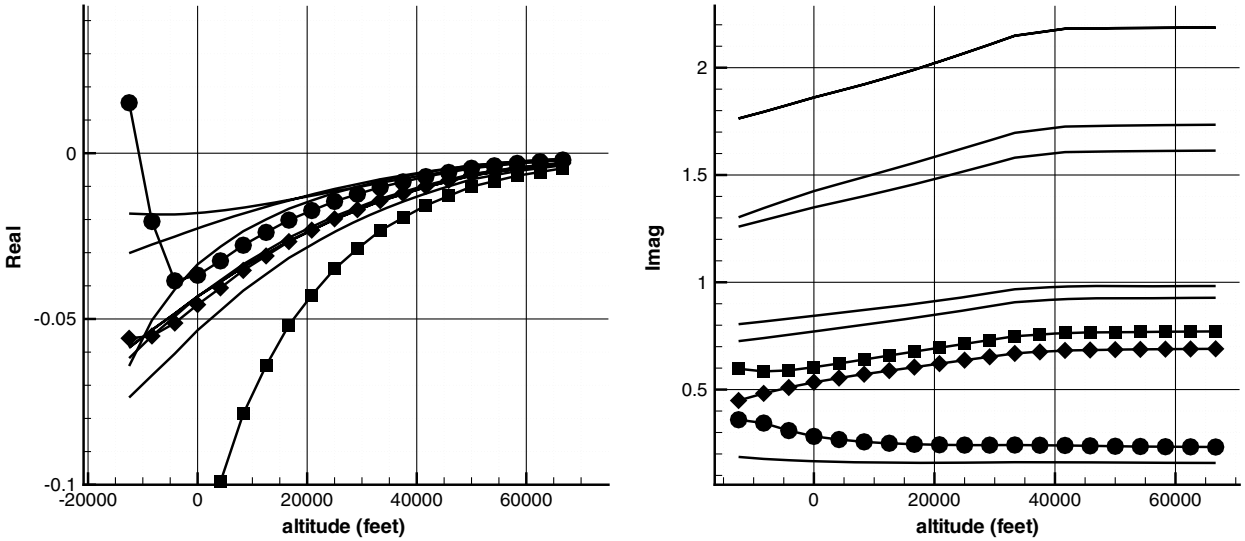

Fig. 12 Variation of real and imaginary parts with altitude for the generic fighter at Mach 0.85.

The structural model consists of three main elements, the wing, leading-edge flap and the aileron, as shown in Fig. 10. These three components are modeled using shell elements with the thickness varying from 3 in. at the root to 2 in. at the tip. It is assumed that the control surfaces are locked and hence these components are linked together via solid connections. The material properties were chosen to be those of aluminum. This gave the first symmetric wing bending mode at 5 Hz and the wing torsion at 16 Hz, which are close to the values for the F-16 clean wing quoted in [19]. To obtain a case that flutters around sea level, the wing was then weakened by reducing Young's modulus by a factor of 2.5. The mode shapes mapped onto the CFD surface grid are shown in Fig. 11.

Calculations were run for Mach numbers between 0.80 and 1.00 in steps of 0.05 and 0 deg angle of attack. At this Mach number a weak shock wave forms over the wing. The correction matrices were calculated and the series approach was used to trace the eigenvalues for altitudes between $-16,667$ ft to 50,000 ft. The steady-state calculation took around 15 min on 32 processors, and the generation of the correction matrix for each mode took around 45 min.

The variation of the real and imaginary parts of the modes is shown for Mach 0.85 in Fig. 12. The symmetric wing bending mode interacts with the symmetric and asymmetric wing torsion modes to produce flutter at about 16,667 ft below sea level.

VI. Conclusions

A new method for computing aeroelastic stability was proposed and demonstrated. The following conclusions are drawn:

1) The use of the Schur complement eigenvalue formulation has allowed large inviscid models to be computed by removing the need to solve large sparse linear systems that are almost singular, as in previous work.

2) The solution of the small nonlinear Schur eigenvalue problem can be done rapidly, meaning that mode tracking using small parameter steps can be used.

3) The series expansion method proved reliable when compared with the nonlinear method.

4) Test cases have been computed for the Goland and MDO wings, SST rudder buzz, and a generic fighter configuration.

5) The cost of computing the eigenvalue loci over the range of altitude varies with the square of the number of modes and is between 5 and 60 times the cost of a steady-state solution for the same problem.

6) The method provides detailed information about the interaction of normal modes, giving insight into the flutter mechanism.

The method described in this paper is being extended in the following ways. First, the term $(A_{ff} - \lambda I)^{-1} A_{fs}$ in the Schur matrix can be generated using forced-motion time-domain calculations. This is being exploited to allow viscous flow models to be used to generate the Schur matrix. Second, the Schur matrix generated for the case with no aerostatic solution can be used to drive the Newton nonlinear solution while including the aerostatic solution for the residual calculation. Third, to reduce the cost of generating the series approximation to the Schur matrix, better approximation methods are being developed, such as kriging approximators used together with sampling techniques.

Acknowledgments

This work is funded by the European Union for the Marie Curie Excellence Team (ECERTA) under contract MEXT-CT-2006 042383.

References

[1] Woodgate, M. A., Badcock, K. J., Rampurawala, A. M., Richards, B. E., Nardini, D., and Henshaw, M. J., "Aeroelastic Calculations for the Hawk Aircraft Using the Euler Equations," *Journal of Aircraft*, Vol. 42, No. 4, 2005, pp. 1005–1012. doi:10.2514/1.5608

[2] Lucia, D. J., Beran, P. S., and Silva, W. A., "Reduced-Order Modeling: New Approaches for Computational Physics," *Progress in Aerospace Sciences*, Vol. 40, No. 1–2, 2004, pp. 51–117. doi:10.1016/j.paerosci.2003.12.001

[3] Thomas, J. P., Dowell, E. H., Hall, K. C., and Denegri, C. M., "An Investigation of the Sensitivity of F-16 Fighter Flutter Onset and Limit Cycle Oscillations to Uncertainties," 47th AIAA/ASME/ASCE/AHS/ASC Structures. Structural Dynamics and Materials Conference, AIAA Paper 2006-1847, Newport, RI, May, 2006.

[4] Morton, S. A., and Beran, P. S., "Hopf-Bifurcation Analysis of Airfoil Flutter at Transonic Speeds," *Journal of Aircraft*, Vol. 36, No. 2, 1999, pp. 421–429. doi:10.2514/2.2447

[5] Badcock, K. J., Woodgate, M. A., and Richards, B. E., "The Application of Sparse Matrix Techniques for the CFD Based Aeroelastic Bifurcation Analysis of a Symmetric Aerofoil," *AIAA Journal*, Vol. 42, No. 5, 2004, pp. 883–892. doi:10.2514/1.9584

[6] Badcock, K. J., Woodgate, M. A., and Richards, B. E., "Direct Aeroelastic Bifurcation Analysis of a Symmetric Wing Based on the Euler Equations," *Journal of Aircraft*, Vol. 42, No. 3, 2005, pp. 731–737. doi:10.2514/1.5323

[7] Woodgate, M. A., and Badcock, K. J., "On the Fast Prediction of Transonic Aeroelastic Stability and Limit Cycles," *AIAA Journal*, Vol. 45, No. 6, 2007, pp. 1370–1381. doi:10.2514/1.25604

[8] Bekas, K., and Saad, Y., "Computation of Smallest Eigenvalues Using Spectral Schur Complements," *SIAM Journal on Scientific Computing*, Vol. 27, No. 2, 2005, pp. 458–481. doi:10.1137/040603528

[9] Eisenstat, S. C., Elman, H. C., and Schultz, M., "Variational Iterative Methods for Nonsymmetric Systems of Linear Equations," *SIAM Journal on Numerical Analysis*, Vol. 20, No. 2, April 1983, pp. 345–357.
doi:10.1137/0720023

[10] Badcock, K. J., Woodgate, M. A., Allen, M. R., and Beran, P. S., "Wing Rock Limit Cycle Oscillation Prediction Based on Computational Fluid Dynamics," *Journal of Aircraft*, Vol. 45, No. 3, 2008, pp. 954–961.
doi:10.2514/1.32812

[11] Saad, Y., and Sosonkina, M., "Parms : A Package for the Parallel Iterative Solution of General Large Sparse Linear Systems User's Guide," Rept. UMSI2004-8, Minnesota Supercomputer Inst., Univ. of Minnesota, Minneapolis, MN, 2004.

[12] Beran, P. S., Knot, N. S., Eastep, F. E., Synder, R. D., and Zweber, J. V., "Numerical Analysis of Store-Induced Limit Cycle Oscillarion," *Journal of Aircraft*, Vol. 41, No. 6, 2004, pp. 1315–1326.
doi:10.2514/1.404

[13] Matsushita, H., Tamayama, M., Saitoh, K., and Nakamichi, J., "NAL SST Arrow Wing with Oscillating Flap," *Verification an Validation Data for Computational Unsteady Aerodynamics*, RTO Technical Report 26, Oct. 2000, pp. 295–318.

[14] Rampurawala, A. M., and Badcock. K. J., "Evaluation of a Simplified Grid Treatment for Oscillating Trailing-Edge Control Surfaces," *Journal of Aircraft*, Vol. 44, No. 4, 2007, pp. 1177–1188.
doi:10.2514/1.24623

[15] Rampurawala. A. M., "Aeroelastic Analysis of Aircraft with Control Surfaces using CFD," Ph.D. Thesis, Univ. of Glasgow, Glasgow, Scotland, U.K., 2006.

[16] Girodroux-Lavigne, P., Grisval, J. P., Guillemot, S., Henshaw, M., Karlsson, A., Selmin, V., et al., "Comparison of Static and Dynamic Fluid-Structure Interaction Solutions in the Case of a Highly Flexible Modern Transport Aircraft Wing," *Aerospace Science and Technology*, Vol. 7, 2003, pp. 121–133.
doi:10.1016/S1270-9638(02)00007-X

[17] Allen, C. B., Jones, D., Taylor, N. V., Badcock, K. J., Woodgate, M. A., Rampurawala, A. M., et al., "A Comparison of Linear and Nonlinear Flutter Prediction Methods: A Summary of PUMA DARP Aeroelastic Results," *The Aeronautical Journal*, Vol. 110, No. 1107, 2006, pp. 333–343.

[18] Goura, G. S. L., Badcock, K. J., and Woodgate, M. A., "Extrapolation Effects on Coupled Computational Fluid Dynamics/Computational Structural Dynamics Simulations," *AIAA Journal*, Vol. 41, No. 2, 2003, pp. 312–314.
doi:10.2514/2.1946

[19] Cattarius, J., "Numerical Wing/Store Interaction Analysis of a Parametric F-16 Wing," Ph.D. Thesis, Virginia Polytechnic Inst. and State Univ., Blacksburg, VA, 1999.

P. Beran
Associate Editor